Physics – Uspekhi **58** (5) 495 – 502 (2015)

CONFERENCES AND SYMPOSIA

PACS numbers: 29.40.Ka, 41.60.Bq, 95.55.Vj

110th ANNIVERSARY OF THE BIRTH OF P A CHERENKOV

Cherenkov detectors for high-energy neutrino astrophysics

Zh-A M Dzhilkibaev, G V Domogatsky, O V Suvorova

DOI: 10.3367/UFNe.0185.201505j.0531

Contents

1. **Introduction** 495
2. **Deep-underwater detection of high-energy particles** 496
   2.1 Vavilov–Cherenkov radiation of charged particles in transparent media; 2.2 Propagation of Cherenkov radiation in a medium
3. **Neutrino telescopes** 498
   3.1 Baikal-GVD; 3.2 KM3NeT; 3.3 IceCube.; 3.4 Astrophysical neutrinos
4. **Conclusion** 501
   References 502

Abstract. This review discusses the current status of and prospects for large-scale Cherenkov detectors that operate in deep-underwater and under-ice environments (Lake Baikal, Mediterranean Sea, Antarctica) and which have, in recent decades, become the primary tool for measuring high-energy neutrino fluxes.

Keywords: Cherenkov radiation, neutrino telescopes, neutrino astrophysics

1. Introduction

Natural neutrinos carry a wealth of information about the surrounding world that might be unique in many respects. Studies of natural neutrino fluxes in different energy bands can provide clues about the evolution of the early Universe, the production of the observed elemental abundance, and the evolution mechanisms of massive stars and supernova explosions. They can also shed light on the dark matter problem, the energy generation mechanism, and the composition and internal structure of the Sun, both at the present time and in the quite distant past, and might even be helpful in the understanding of one of the most difficult objects for study — the planet Earth.

Putting aside the "problem of the century" (after A D Sakharov) — the detection of relic neutrino radiation, which now seems to be a remote dream — the remainder of the energy range under study shown in Fig. 1 can be conditionally split into three categories by the neutrino registration methods applied. In the energy range from 10^5 to 10^9 eV, all the results have been obtained in underground laboratory experiments using either radio-chemical (chlorine–argon, gallium–germanium) methods of neutrino detection, or liquid-based or plastic-based scintillation detectors, or water Cherenkov detectors. The biggest Cherenkov detector, SuperKamiokande (Japan), with a working volume of purified water of 22.5 thousand cubic meters has detected neutrino fluxes with an energy of $10^8 - 10^9$ eV, which are produced by cosmic rays in Earth's atmosphere, and discovered neutrino oscillations.

The upper boundary of the next energy range ($10^9 - 10^{16}$ eV) is rather uncertain, because neutrinos in this energy range are primarily studied by large-scale Cherenkov detectors (neutrino telescopes) constructed in natural environments (natural water reservoirs and Antarctic ice), and there are prospects to further increase the sensitivity of such

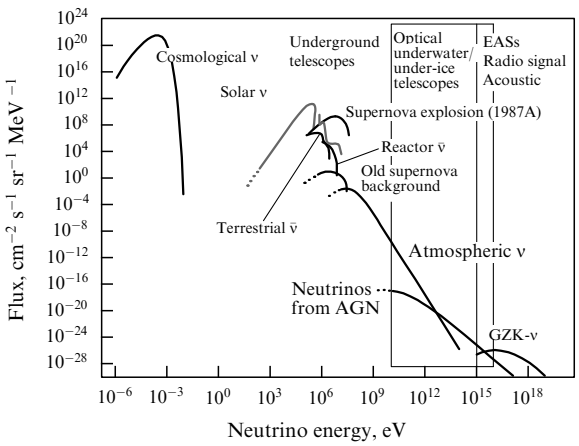

Figure 1. Natural neutrino fluxes on Earth and their detection methods: AGN — active galactic nuclei, GZK — Greizen–Zatsepin–Kuzmin cutoff of ultrahigh-energy cosmic rays, ν — neutrino, and ν̄ — antineutrino.

Zh-A M Dzhilkibaev, G V Domogatsky, O V Suvorova Institute for Nuclear Research, Russian Academy of Sciences,
prosp. 60-letiya Oktyabrya 7a, 117312 Moscow, Russian Federation
E-mail: domogats@pcbai10.inr.ruhep.ru, suvorova@cpc.inr.ac.ru

Received 16 March 2015
Uspekhi Fizicheskikh Nauk **185** (5) 531 – 539 (2015)
DOI: 10.3367/UFNr.0185.201505j.0531
Translated by K A Postnov; edited by A Radzig

detectors. This method of experimental neutrino astrophysics, proposed in 1960 by the outstanding Soviet physicist M A Markov [1], turned out to be extremely fruitful. To date, the method of deep-underwater detection of elementary particles (and its modification for Antarctic ice) has been well developed. The first detectors were constructed at Lake Baikal, at the South Pole in Antarctica (AMANDA — Antarctic Muon And Neutrino Detector Array), and in the Mediterranean Sea (ANTARES — Astronomy with a Neutrino Telescope and Abyss environmental RESearch). Finally, IceCube Neutrino Observatory, presently the biggest installation, with a working volume of 1 km^3 of Antarctic ice, is at work, at which high-energy astrophysical neutrinos were first detected in 2010–2013. The energy of the most powerful of these events is estimated to be about 2×10^{15} eV. Diffuse neutrino flux is currently being studied at a sensitivity level that is three orders of magnitude higher than the sensitivity of the biggest underground detectors.

Hopes to probe fluxes of neutrinos with energies above $10^{17} - 10^{18}$ eV are usually related to the development of the acoustic methods of neutrino detection and to the construction of detectors with a huge volume in natural water reservoirs, or to studies of extensive air showers using giant ground-based installations, or to the development of the method of radio signal detection from neutrinos.

The purpose of the present paper is to highlight some features of the deep-underwater method of a Cherenkov radiation detection, to report on the state of the art and prospects of the construction of large-scale Cherenkov detectors in natural environments, and to discuss current research with these detectors.

2. Deep-underwater detection of high-energy particles

As noted in the Introduction, natural high- and ultrahigh-energy neutrino fluxes can be probed by deep-underwater (under-ice) neutrino telescopes, which register Cherenkov radiation from secondary muons and electromagnetic or hadron showers, which are produced by neutrino interactions, using a set of photodetectors located at quite large distances — from several dozen to several hundred meters — from each other. The efficiency of this detection method is largely determined by both the characteristic features of Cherenkov radiation from charged particles and the hydro-optical properties of the medium in which the experiment is carried out.

2.1 Vavilov–Cherenkov radiation of charged particles in transparent media

A charged particle moving in a refracting medium with a velocity exceeding the speed of light in the medium emits Cherenkov radiation [2]. The spectral distribution of Cherenkov photons emitted from a unit length of the particle's trajectory with a unitary charge is given by the following relationship

$$\frac{\mathrm{d}n_{\mathrm{C}}}{\mathrm{d}\lambda} = 2\pi\alpha\left(1 - \frac{1}{\beta^2 n^2}\right)\frac{1}{\lambda^2}\,, \tag{1}$$

where λ is the photon wavelength in cm, $\alpha \approx 1/137$ is the fine-structure constant, $n(\lambda)$ is the phase refraction index of the medium, and $\beta = v/c$ is the relative velocity of the particles in units of the speed of light in vacuum. A remarkable feature of Cherenkov radiation, which largely determines the efficiency of the deep-underwater method of particle detection, is the emission of Cherenkov photons at each instant of time from the point on the particle's trajectory under the fixed angle θ_{C} relative to the particle's velocity. The Cherenkov angle θ_{C} is defined as $\cos\theta_{\mathrm{C}} = 1/(\beta n)$ and is about 42° in water or ice. The absolute value of the velocity $v_{\mathrm{C}}(\lambda)$ of Cherenkov photons is determined by the group velocity of the light propagation with the corresponding wavelength in the medium:

$$v_{\mathrm{C}} = \frac{c}{n_{\mathrm{g}}(\lambda)}\,, \quad n_{\mathrm{g}}(\lambda) = n(\lambda) - \lambda\,\frac{\mathrm{d}n}{\mathrm{d}\lambda}\,. \tag{2}$$

The working range of photons detected in deep-underwater experiments spans 350–600 nm. The lower boundary of this range is determined by light absorption in the photodetector glass, and the upper boundary is due to the light absorption increase in water and ice and the decrease in the Cherenkov radiation intensity and the quantum sensitivity decay of electronic photomultipliers as the wavelength of photons in the red part of the spectrum increases. The group velocity of light propagation in water and ice increases with the photon wavelength, which spreads the Cherenkov radiation signal in time.

Muons and showers with energies of several hundred GeV and above represent two different sources of the high-intensity Cherenkov radiation detected by neutrino telescopes.

2.1.1 High-energy showers. Showers with high energies are produced by the interaction of a neutrino (ν) with nucleons (N) in the reactions

$$\nu_l(\bar{\nu}_l) + \mathrm{N} \overset{\mathrm{CC}}{\to} l^-(l^+) + \text{hadrons}\,,$$
$$\nu_l(\bar{\nu}_l) + \mathrm{N} \overset{\mathrm{NC}}{\to} \nu_l(\bar{\nu}_l) + \text{hadrons}\,,$$

where $l = \mathrm{e}$, μ, or τ, CC is the charged current, and NC is the neutral current, as well as during the resonance scattering of an electron antineutrino on an electron:

$$\bar{\nu}_{\mathrm{e}} + \mathrm{e}^- \to \mathrm{W}^- + \ldots\,,$$

with the resonance energy $E_0 = M_{\mathrm{W}}^2/2m_{\mathrm{e}} = 6.3 \times 10^6$ GeV and the interaction cross section of 5.02×10^{-31} cm^2. The Cherenkov radiation of electromagnetic and hadron showers is formed by photons emitted by charged particles of the shower (mainly by electrons and positrons) and is determined by their spatial, angular, and time distributions. The lateral size of the electromagnetic shower, which is characterized by the Moliére radius (about 9 cm for water), has virtually no effect on the response of the neutrino telescope photodetectors. The angular distribution of the electron component of the shower weakly changes along the shower axis near the maximum of the cascade curve, where most of the Cherenkov photons are originated, and for showers with energies above 100 GeV this angular distribution can be satisfactorily described by the unified function $\Psi_{\mathrm{e}}(\theta)$ independent of the space coordinates. Thus, the distribution of the shower electron component can be presented in the form

$$N_{\mathrm{e}}(x, \rho, \theta, t) \approx N_{\mathrm{e}}(x)\,\Psi_{\mathrm{e}}(\theta)\,\delta\left(t - \frac{x}{c}\right), \tag{3}$$

where c is the speed of light in vacuum.

The number of Cherenkov photons $N_C(x,\theta,t)\,dx\,d\mathbf{\Omega}\,dt$ emitted from an interval with length dx at the point x into the solid angle element $d\mathbf{\Omega}$ is proportional to the total length of the charged particle trajectories over the interval dx. Since most of the shower particles move along its axis, one finds approximately $dl_e \approx N_e(x)\,dx$. The relative angular distribution of Cherenkov photons, summed over all the trajectories of charged particles in the shower, $\Psi_C(\theta)$ (Fig. 2) [3], is virtually independent of the shower energy for $E_{sh} > 100$ GeV. The angular distributions of Cherenkov photons emitted from different parts of the shower axis in the vicinity of the cascade curve maximum differ insignificantly from the total distribution $\Psi_C(\theta)$ [4], which enables one to separate the angular and space variables and to represent N_C in the form

$$N_C(x,\theta,t) \approx N_e(x)\,n_C\Psi_C(\theta)\,\delta\left(t-\frac{x}{c}\right), \tag{4}$$

where n_C is the linear density of Cherenkov radiation of relativistic particles (for water and ice, $n_C \approx 230-240$ photons per cm in the wavelength range of 350–600 nm).

The development of an air shower can be most completely reproduced by Monte Carlo simulations. However, this procedure requires a lot of computational time. Therefore, to model the response of neutrino telescopes to the Cherenkov radiation from showers, it is appropriate to take advantage of analytical approximations of the transverse distribution of charged particles in electromagnetic and hadron showers. For example, one of the approximations proposed by Belen'kii [5], reads as follows:

$$N_e(X) = \left(\frac{E_{sh}}{E_C}\right)^S S^{-1.5X}\exp\left(-2.49S+0.5(S-1)\,X+0.025\right), \tag{5}$$

$$S = \frac{3X}{X+2\ln\left(E_{sh}/E_C\right)-2.4}, \tag{6}$$

where $E_C = 72$ MeV, $X = x/x_0$, and $x_0 = 36.1$ cm is the radiation length for water.

The development of an electromagnetic shower is determined by the bremsstrahlung cross section of electrons and by the e^+e^--pair production cross section by photons. As was first pointed out by L Landau and I Ya Pomeranchuk and then justified quantum-mechanically by Migdal [6] the bremsstrahlung and e^+e^--pair production cross sections in a dense medium can be reduced by the factor $E^{-1/2}$ for high enough energies of electrons and photons due to their collective interaction with atoms of the medium [Landau–Pomeranchuk–Migdal (LPM) effect]. The LPM effect becomes significant in water at electron and photon energies above $E_{LPM} \approx 2240$ TeV [7].

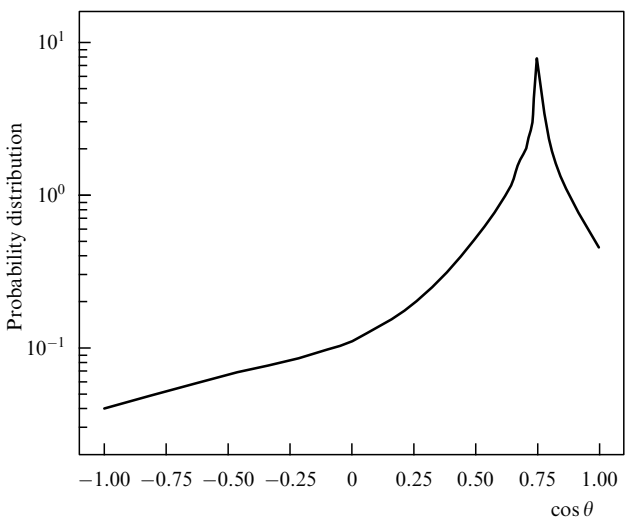

Figure 2. Cherenkov radiation from electromagnetic high-energy air showers integrated over all $e^\pm$ trajectories.

The characteristic influence of the LPM effect on the development of electromagnetic showers can be formulated as follows [8]. For energies exceeding E_{LPM}, the longitudinal size of the shower increases. The LPM effect does not really affect the total length of the shower particle trajectories, which remains proportional to shower energy. The particle distribution near the shower maximum is significantly broader than when the LPM effect is ignored, but the number of particles in the maximum decreases. The deviation of the form of the longitudinal distribution $N_e(x)$ from the case of ignoring the LPM effect becomes significant starting at energies on the order of $10E_{LPM} \approx 20$ PeV. Above this energy, the shower increases in size with energy as $E_{sh}^{1/3}$. The influence of the LPM effect on the development of hadron showers produced by neutrino interactions becomes significant only for $E_{sh} > 1$ EeV [9, 10].

The total number of Cherenkov photons from an electromagnetic or a hadron shower is proportional to the total length of charged particle trajectories and, correspondingly, to the shower energy:

$$N_C^{tot} = n_C L_C = BE_{sh}\ [\text{GeV}]\,. \tag{7}$$

In the case of an electromagnetic shower, the proportionality coefficient is [4, 11]

$$B = (1.04-1.16)\times 10^5 \text{ photons per GeV}\,, \tag{8}$$

and for a hadron shower one has [10]

$$B = 0.86\times 625 f(\epsilon)\,n_C\,,\quad \epsilon = \log\left(E_{sh}\ [\text{TeV}]\right), \tag{9}$$

$$f(\epsilon) = -1.27\times 10^{-2} - 4.76\times 10^{-2}(\epsilon+3) - 2.07\times 10^{-3}(\epsilon+3)^2 + 0.52\sqrt{\epsilon+3}\,,$$

where the numerical factor 0.86, according to Ref. [11], takes into account the decrease in n_C for nonrelativistic electrons in a hadron shower. Bearing in mind formula (7), the number of Cherenkov photons emitted by the shower axis segment Δx in the neighborhood of point x can be presented in the following form:

$$N_C(x,\Delta x,\theta,t) = BE_{sh}\Psi_C(\theta)\,\delta\left(t-\frac{x}{c}\right)\int_{x-\Delta x/2}^{x+\Delta x/2}\overline{N}_e(x')\,dx'\,, \tag{10}$$

where $\overline{N}_e(x)$ is the distribution of the electron component along the shower axis, which is normalized to unity. One of the possible algorithms of modeling Cherenkov radiation from high-energy showers can be formulated as follows. The longitudinal length of a shower is split into sufficiently small segments Δx, and the shower is treated as a superposition of point-like sources of Cherenkov radiation located at the center of each segment with intensity $N_C(x,\Delta x,\theta,t)$ determined by relationship (10).

2.1.2 Muons. Muon energies probed by neutrino telescopes span the range from a few dozen GeV to ultrahigh energies. The radiation flux emitted by a muon passing through a medium includes Cherenkov radiation initiated by the muon's electric charge, Cherenkov radiation of δ-electrons produced by the atomic ionization of the medium by the muon, and Cherenkov radiation from showers generated due to e^+e^--pair production or due to bremsstrahlung and photonuclear interactions of the muon with a medium.

Thus, the radiation field initiated by a muon in the medium can be separated into two components. The first component emits continuously with a constant linear density determined by expression (1) during the muon motion along its trajectory. The linear density and angular distribution of photons in this source are due to Cherenkov photons emitted by the muon itself. The second component, which is formed by local (in the rough approximation, point-like) sources along the muon trajectory, describes Cherenkov radiation from showers generated by e^+e^--pair production, as well as due to bremsstrahlung and photonuclear muon interactions (see Section 2.1.1).

2.2 Propagation of Cherenkov radiation in a medium

The main optical parameters of a medium that determine the propagation of Cherenkov radiation of muons and showers in natural media include the absorption coefficient $\kappa(\lambda)$, the scattering coefficient $\sigma(\lambda)$, and the scattering indicatrix $\chi(\mu, \lambda)$, where $\mu = \cos\theta$, and θ is the scattering angle of a photon. Figure 3 shows the characteristic spectral dependences of the optical parameters of the medium at the sites of deep-underwater experiments in Lake Baikal, the South Pole in Antarctica, and the Mediterranean Sea.

The Antarctic ice is characterized by a strong inhomogeneity with the depth, which is due to the different transparency of the atmosphere and different formation conditions of the Antarctic snow shield over a period of about 10 thousand years. As a result, the light absorption length in the ice at depths from 1500 to 2500 m varies in a wide range from 30 m to 150 m, the scattering length changes from 0.4 m to 4 m, and the effective scattering length does not exceed 30 m. The intense scattering of light in combination with its weak absorption in the Antarctic ice result in the rapid isotropization of the light field and, correspondingly, in the loss of information about the coordinates and the orientation of the source of Cherenkov radiation.

The optical properties of deep waters of the Mediterranean Sea are characterized by the light absorption length of 40–70 m, and the scattering length of about 30–60 m.

For the deep Baikal waters, the absorption length ranges 22–25 m, and the scattering length 30–50 m.

The light scattering length in the Baikal and Mediterranean waters is about two orders of magnitude larger than in the Antarctic ice. Because of this, the deep-underwater telescopes Baikal-GVD (Baikal Gigaton Volume Detector) and KM3NeT (KM3 Neutrino Telescope) would have significant advantages in studies of the diffuse neutrino flux at energies varying from 10^2 to 10^6 TeV. These telescopes would be able to probe both the neutrino energy spectrum at the sensitivity level of the IceCube detector and to study the global and local anisotropies of the diffuse neutrino flux by detecting showers produced by neutrinos of all three flavors with the subsequent retrieval of the shower axis orientation with an accuracy of about $1^\circ - 3^\circ$. Notice that the accuracy of the shower axis reconstruction by the IceCube detector is less than 15°.

3. Neutrino telescopes

The history of the appearance and development of experimental neutrino astronomy is described in detail in reviews [12, 13]. Until recently, our knowledge about the natural high- and ultrahigh-energy neutrino fluxes came from the Cherenkov neutrino detectors HT200/HT200+ [14] and AMANDA, as well as ANTARES neutrino telescope, which

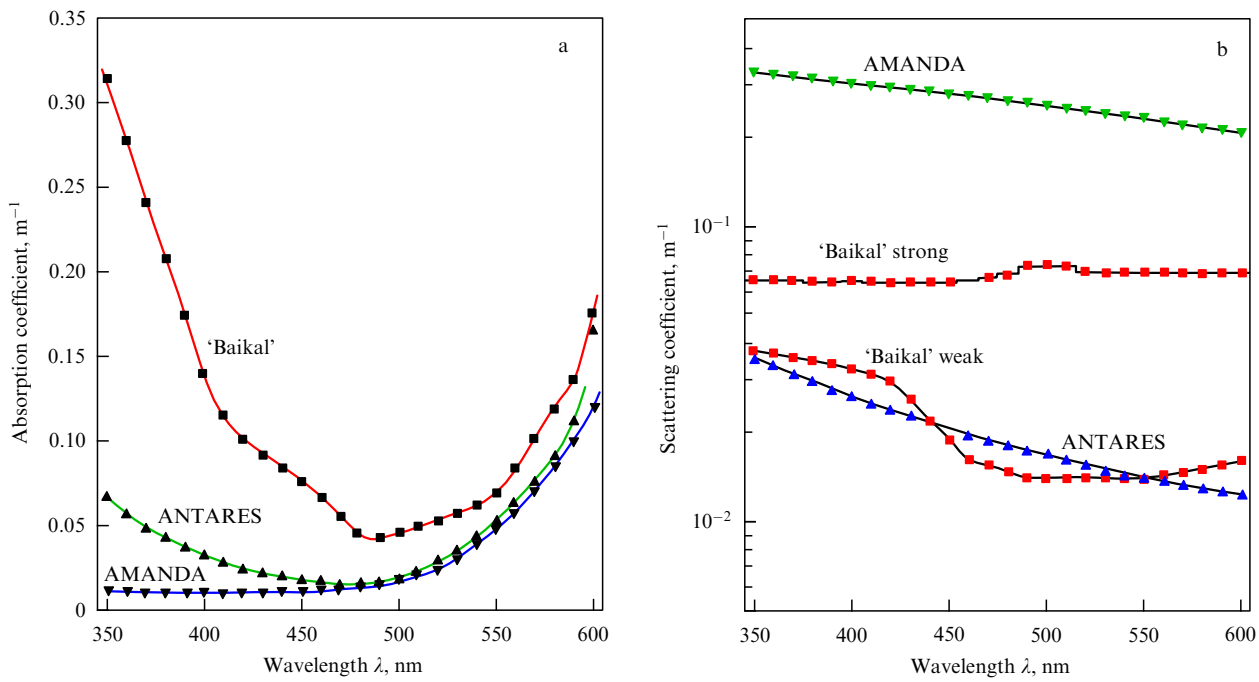

Figure 3. Spectral dependence of the absorption coefficient (a), and scattering coefficient (b) in the Baikal water, Antarctic ice, and Mediterranean water.

has been taking data since 2008. These three installations, which belong to the first-generation neutrino telescopes, are characterized by an effective volume for the secondary muon and shower detection of order 10^7 m^3 relative to the registration of neutrinos with energies above 10 TeV.

The successful operation of first-generation neutrino telescopes over more than decade (starting from the end of the 1990s) and sensitivities to the high-energy natural neutrino fluxes reached by these detectors, which are about two orders of magnitude higher than the sensitivities in the largest underground experiments [SuperKamiokande, and MACRO (Monopole, Astrophysics and Cosmic Ray Observatory)], have clearly demonstrated the possibility of applications and the efficiency of the neutrino detection method in natural environments. The results obtained in these experiments motivated the design and construction of neutrino telescopes with a characteristic scale of about 1 km^3 and sensitivity to high-energy natural neutrino fluxes by an order of magnitude higher than existing devices.

Presently, three large-scale second-generation neutrino telescopes operating in natural surroundings are under construction: the IceCube project at the South Pole, KM3NeT in the Mediterranean Sea, and Baikal-GVD in Lake Baikal, which are currently at different stages of realization. The configuration, architecture of measurement and communication systems of these detectors, as well as possibilities of solving concrete tasks, are determined by their specific location, environmental properties, degree of complexity of technical-engineering design of the installations and their exploitation, expenses for creating and maintaining the infrastructure, and possibility of modifying their configuration and increasing the telescope power.

3.1 Baikal-GVD

In 2006-2010, the 'Baikal' Collaboration designed, manufactured, and tested in natural conditions at Lake Baikal the prototypes of all basic units and systems of the Baikal-GVD telescope, and the Baikal-GVD telescope scientific-technical project was designed [15]. The telescope will have a module structure consisting of functionally independent facilities — clusters of vertical strings of optical modules (Fig. 4). The module structure will allow experimental data to be taken already at the commissioning phase and will have the capacity to almost infinitely increase its volume and adapt (upon changing the research priorities) its configuration to specific scientific tasks.

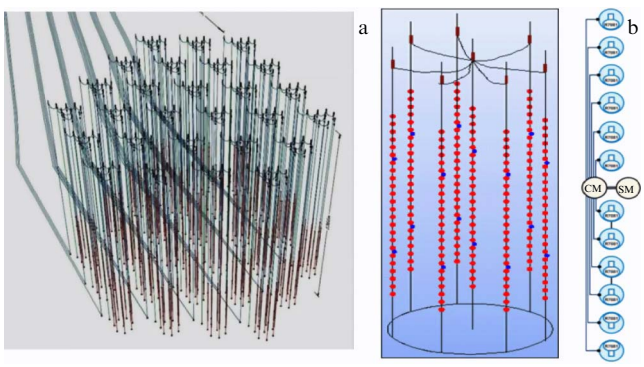

Figure 4. Schematic view of the Baikal-GVD neutrino telescope (a) and a cluster of the telescope (b). One section of the cluster is shown in the right fragment of figure b.

Hamamatsu-R7081HQE photoelectric multipliers (PEMs) with semispherical photocathodes 250 mm in diameter and high quantum efficiency are the main detecting devices of Baikal-GVD. PEMs together with controling electronics are located in deep-underwater glass shells which form optical modules (OMs). The optical modules are mounted on vertical load-carrying cables that form strings (garlands). The section of optical modules is the main structural unit of a string. The section represents a functionally completed unit of the detector, including the signal registration, processing, calibration, trigger formation, and data transmission systems. Each section contains 12 optical modules spaced 15 m apart along the string, as well as a central module (CM) and service module (SM).

Analog signals from all OMs of a section are transmitted to the CM along coaxial cables with equal lengths. These cables also provide a low-voltage power supply of OMs. In CMs, the analog signals from optical modules are converted into a digital code, and the information is further transmitted using an Ethernet line. The service module is destined for calibrating the time channels of the installation, for supplying power to the OMs, and for determining the position of the string relative to the bottom beacons. The location of the string is determined by a hydroacoustic positioning system.

The synchronization, electric power supply, and data transmission channels of the sections are united in the commutation module of the string. This module is connected with cable lines $\approx$ 1200 m in length with the central control unit of the cluster. The basic configuration of the cluster includes eight (one central and seven peripheral) strings. Each string consists of 24 OMs (two sections per string). Strings are spaced $\approx$ 60 m apart. The clusters of strings are connected with the shore center by combined electro-optical communication lines with a length of about 6 km.

In 2011, the final stage of complex tests and adjustments of the elements and systems of the Baikal-GVD telescope commenced, and is to be completed in 2015 with the construction of the multimegaton deep-underwater neutrino detector consisting of 192 photodetectors attached to eight vertical strings — the first demonstration cluster of the Baikal-GVD neutrino telescope. The volume and sensitivity of this installation will be comparable to those of the neutrino telescope ANTARES in the Mediterranean Sea, presently the biggest in the northern hemisphere. In 2014, a deep-underwater unit comprising 112 optical modules attached to five strings of the first cluster was installed in Lake Baikal. The next phase of the development of the Baikal-GVD detector is the construction by 2020 of the first stage of the telescope consisting of 12 clusters with a volume of about 0.5 km^3, which is comparable to the IceCube detector volume, for detection of astrophysical neutrinos. The second stage of the telescope will include 27 clusters with a total volume of about 1.5 km^3.

3.2 KM3NeT

The main participants of the KM3NeT project, which is aimed at constructing a cubic-kilometer scale neutrino telescope in the Mediterranean Sea, include the ANTARES collaboration (France, Italy, Netherlands, etc.) and the NEMO (Neutrino Mediterranean Observatory, Italy) and NESTOR (Neutrino Extended Submarine Telescope with Oceanographic Research, Greece) Collaborations. In 2006–2010, the general concept of the future telescope was

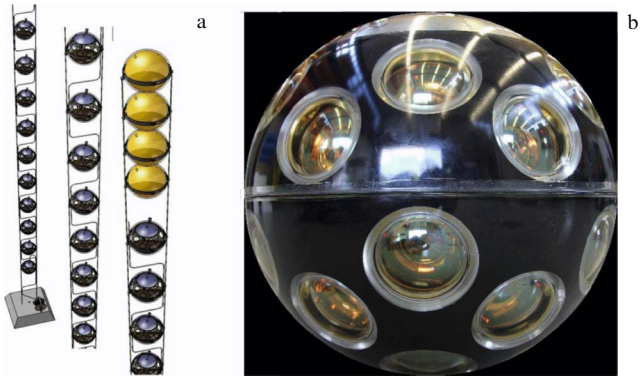

Figure 5. (a) String of optical modules. Shown are the bottom, middle, and top parts of the string. (b) The optical module of the KM3NeT experiment.

elaborated and several alternative variants of its main elements and system were examined [16].

The telescope will have a dispersed infrastructure consisting of 4–6 blocks, each constituting a full-scale neutrino telescope with a volume of 0.5–0.8 km^3 each. These blocks will be located in three geographic regions: in Toulon Bay (KM3NeT_Fr, France), near Sicily (KM3NeT_It, Italy), and near the city of Pilos (KM3NeT_Gr, Greece). Each of these regions will see the deployment of two blocks, each comprising 115 strings of optical modules spaced 90–120 m apart. Each string (Fig. 5a) includes 18 optical modules attached sequentially along the string with a separation of 36 m from each other. The lowermost module of the string will be placed 100 m above the sea bottom. The optical module consists of 31 small-sized PEMs with a diameter of $\approx$ 7.6 cm, which are put inside a glass sphere 43.2 cm in diameter (Fig. 5b). All information from each optical module is transmitted directly to the shore control and data taking center via an optical fiber communication line.

In April 2013, long-term natural tests of the working version of the optical module included in the ANTARES telescope were commenced. In April 2014, a working prototype of the string with three optical modules was deployed close to Sicily shore.

Future plans on the realization of the KM3NeT project assume the development of the shore and underwater infrastructure of the telescope in France and Italy and the deployment, by the end of 2016, of 31 strings of the telescope (24 in Italy, and 7 in France). The next stage of the project stipulates the installation in 2017–2018 of two blocks (one in France, and one in Italy) with a total volume of about 1–1.6 km^3, which would enable searches for astrophysical neutrinos registered in the IceCube experiments. The final goal of the project is the construction of the telescope, consisting of six blocks with a total volume of 3–5 km^3, depending on the chosen spacing between strings.

3.3 IceCube

The IceCube neutrino telescope is located at the Amundsen–Scott South Pole Station in Antarctica at a depth of 1450–2450 m under the surface and is a large array of 5160 optical sensors attached to 86 strings (Fig. 6) [17].

Eighty strings of the telescope 125 m apart each includes 60 optical modules attached along the string with a spacing of 17 m. On the surface of the ice immediately above the

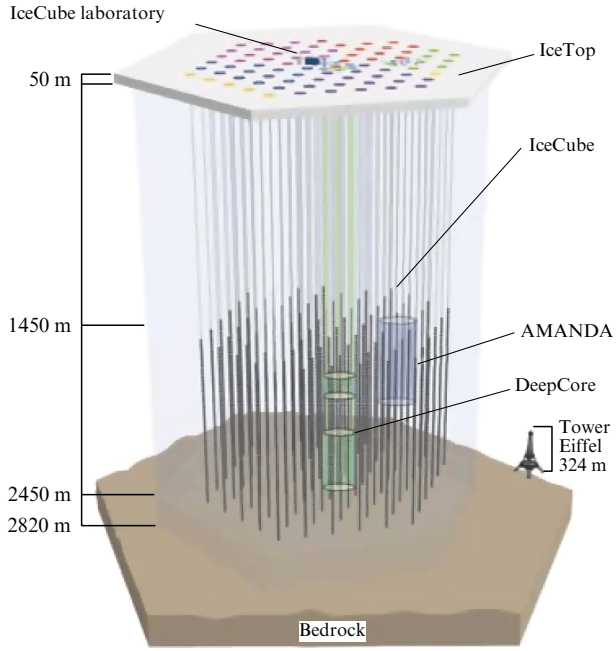

Figure 6. Schematic view of the IceCube neutrino telescope. Shown are the AMANDA detector, the central part of the telescope with a larger number of optical sensors (DeepCore), and the surface IceTop detector of extensive air showers.

neutrino telescope, 320 optical sensors are installed, which form the on-ice IceTop detector to register the particles of extensive air showers. To increase the sensitivity of the telescope in experiments on neutrino oscillations and searches for new particles (dark matter particle candidates), as well as to increase the aperture of the telescope for registration of neutrinos from the upper hemisphere, the density of photodetectors in the central part of the telescope, which was called the DeepCore, is increased by means of the installation of six additional strings 72 m in length with a denser location of sensors along them. DeepCore has a sensitivity volume of about 10^7 m^3 with a muon registration energy threshold on the order of 10 GeV.

The first of 86 strings of IceCube was deployed at the South Pole in winter 2005. In subsequent years, the rate of the construction of the detector increased, so that the detector started running in the project configuration in February 2011. The analysis of the experimental data collected during both the commissioning phase and first runs led to important results in searches for astrophysical neutrinos, detection of neutrino fluxes accompanying gamma-ray bursts, searches for dark matter manifestations, and studies of the diffuse neutrino flux, and in some other problems.

The immediate plans of developing of the infrastructure of the IceCube telescope include the elaboration of a low-energy neutrino detector with a muon registration energy threshold of about 1 GeV and an effective volume of 1–10 Mt [Precision IceCube Next-Generation Upgrade (PINGU) detector] by means of a further increase in the number density of sensors in the central part of the DeepCore telescope attached to additional strings. One of the main tasks of the PINGU detector consists in determining the neutrino mass hierarchy from an analysis of the energy and angular distributions of muons from atmospheric muon neutrinos and antineutrinos detected by the telescope. The other direction of development

of the South Pole neutrino observatory also assumes the elaboration of a project of a new detector with a volume of 7–10 km^3 to study fluxes of neutrinos at energies above 1 PeV.

3.4 Astrophysical neutrinos

Presently, searches for astrophysical neutrinos in the Ice Cube experiment [18] may lead to the most striking and significant results for future development of neutrino astrophysics. The neutrino events were selected from the interactions of neutrinos with energies above 30 TeV inside the inner part of the telescope with a volume of about 0.4 km^3. From the analysis of data collected over three years from May 2010 until May 2013 (including 988 days of 'living time' of the detector), 37 events were selected, which corresponds to a 5.7σ excess above the expected number of background events from atmospheric muons and neutrinos. The numbers of background events from atmospheric muons and neutrinos are 8.4 ± 4.2 and $6.6(-1.6 + 5.9)$, respectively. Of this sampling, three events have energies of above 1 PeV. The relative fraction of the air shower events (28) and events with a muon track (9 events) among the total number of events is consistent with the expected fraction of such events in a flux with equal fractions of neutrinos with different flavors. The accuracy of retrieval of the directions of muons and air showers in this analysis is estimated as $\leqslant 1^\circ$ and $\geqslant 15^\circ$, respectively. The reconstructed directions of muon and air shower events are in agreement with the isotropic distribution of incoming neutrinos. Figure 7 plots the distribution of the detected events by energy released in the telescope, as well as the distributions of expected background events.

The energy distribution of experimental events is consistent with the power-law behavior of astrophysical neutrino spectrum with a power index of -2.3 ± 0.3. The position of the reconstructed neutrino incoming directions on the celestial sphere is shown in Fig. 8 in galactic coordinates.

An analysis of data has not revealed the statistically significant clustering of neutrino events in the sky. Presently, the low volume of statistics and insufficient accuracy of the direction reconstruction of the shower events in IceCube does not allow one to uniquely discriminate between the galactic and extragalactic nature of the observed neutrino sources. From this point of view, the construction of the Baikal-GVD and KM3NeT water neutrino telescopes, which are capable of reconstructing shower events with an accuracy of about several degrees, will allow significant advances in the solution to this problem.

The results obtained by the IceCube experiment are a very important milestone in studies of natural fluxes of high-energy neutrinos. They allow measurements of astrophysical neutrino fluxes and determine the required sensitivity level in high-energy neutrino astrophysics.

4. Conclusion

The possibility of detecting the Cherenkov glow from products of neutrino interactions in water in combination with its experimental realization in natural water reservoirs (lakes, seas, oceans) and the Antarctic ice has resulted in the development of deep-underwater experimental high-energy neutrino astrophysics. Practical realization of this seemingly obvious method has required that many quite nontrivial deep-underwater engineering problems be solved, which are related to the construction of control systems of installations consisting of spatially separated units, the development of deep-underwater high-speed data transmission systems, and the solution of the specific data processing and data analysis tasks.

The successful operation of the first-generation detectors, such as HT-200, AMANDA, ANTARES, and, finally, of the present-day 'masterpiece' detector, IceCube, with a working volume of a cubic kilometer scale, has led the scientific community to realize that further development of detectors is required. Specifically, the coordination and joint agreement of future plans of the existing detectors and the design of the

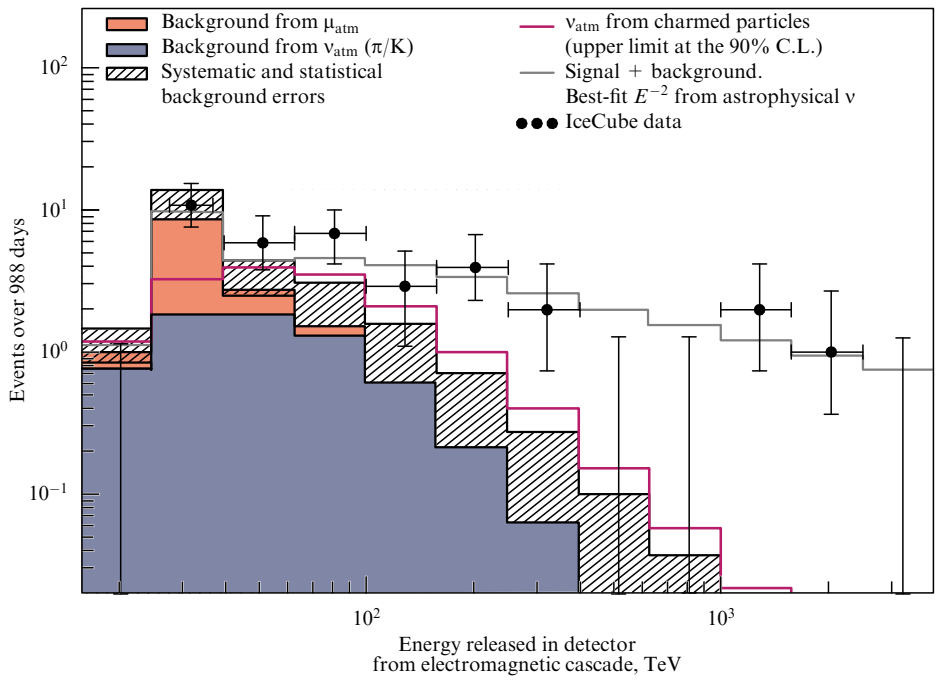

Figure 7. (Color online). Energy deposit in detected events and the expected energy distributions from atmospheric muons (μ_{atm}) and neutrinos (ν_{atm}).

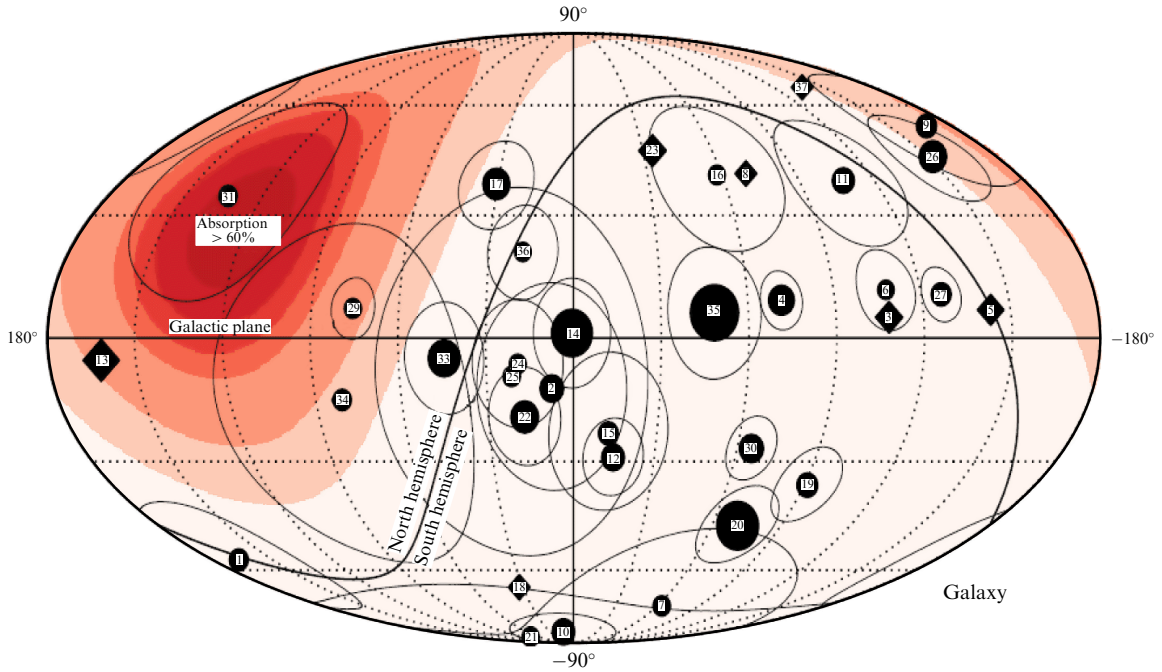

Figure 8. Incoming directions of neutrino events with energies above 30 TeV on the celestial sphere (in galactic coordinates). All 28 'cascade events' (filled circles) and 7 'track events' (filled diamonds) are shown. The symbol size is scaled with the energy of the event from 30 TeV to 2 PeV. The angular uncertainty in reconstructing the incoming directions of cascade events corresponds to the size of elliptical contours around the symbols of events [18].

Global Neutrino Network (GNN) as the first step in the construction of the Global Neutrino Observatory (GNO) consortium are needed. GNO will include all existing international collaborations — ANTARES, Baikal, IceCube, and KM3NeT. The development of this joint collaboration should increase the reliability and significance of the results obtained, facilitate the solution of technical problems, and allow searches for high-energy neutrino events in the whole sky.

The work related to the Baikal neutrino project was supported by the Russian Foundation for Basic Research (grants 13-02-12221ofi-m, 14-02-00972a, and 15-02-10125k).

References

1. Markov M A, in *Proc. of the 1960 Annual Intern. Conf. on High Energy Physics at Rochester* (Eds E C G Sudarshan, J H Tinlot, A C Melissinos) (Rochester, N.Y.: Univ. of Rochester, 1960) p. 578
2. Tamm I E, Frank I M *C.R. Acad. Sci. USSR* **14** 107 (1937); *Dokl. Akad. Nauk SSSR* **14** 107 (1937); *Usp. Fiz. Nauk* **93** 388 (1967); Tamm I *J. Phys. USSR* **1** 439 (1939); Translated into Russian: *Sobranie Nauchnykh Trudov* (Collected Scientific Work) Vol. 1 (Moscow: Nauka, 1975) p. 77
3. Belyaev A, Ivanenko I, Makarov V, in *Proc. of the 1978 DUMAND Summer Workshop, La Jolla, Calif., July 24 – September 2, 1978* Vol. 1 (Eds A Roberts, G A Wilkins) (La Jolla, Calif.: DUMAND, Scripps Institution of Oceanography, 1979) p. 337
4. Bezrukov L B, Butkevich A V, in *Simulation and Analysis Methods for Large Neutrino Telescope. Proc. of the Workshop, Zeuthen, Germany, July 6 – 9, 1998* (DESY-PROC-1999-01, Ed. Ch Spiering) (Zeuthen: DESY, 1999) p. 265
5. Belen'kii S Z *Lavinnye Protsessy v Kosmicheskikh Luchakh* (Avalanche Processes in Cosmic Rays) (Moscow–Leningrad: Gostekhizdat, 1948)
6. Migdal A B *Phys. Rev.* **103** 1811 (1956)
7. Dovzhenko O I, Pomanskii A A *Sov. Phys. JETP* **18** 187 (1964); *Zh. Eksp. Teor. Fiz.* **45** 268 (1963)
8. Alvarez-Muñiz J, Zas E *Phys. Lett. B* **411** 218 (1997)
9. Alvarez-Muñiz J, Zas E, astro-ph/9906347
10. Alvarez-Muñiz J, Zas E *Phys. Lett. B* **434** 396 (1998)
11. Wiebusch Ch H V, PhD Thesis (Aachen: Physikalische Inst. RWTH, 1995)
12. Spiering Ch *Eur. Phys. J. H* **37** 515 (2012)
13. Katz U F, Spiering Ch *Prog. Part. Nucl. Phys.* **67** 651 (2012); arXiv:1111.0507
14. Domogatsky G V *Phys. Usp.* **54** 949 (2011); *Usp. Fiz. Nauk* **181** 984 (2011)
15. The 'Baikal' Collab., Nauchno-Tekhnicheskii Proekt Glubokovodnogo Neitrinnogo Teleskopa Kubokilometrovogo Masshtaba na oz. Baikal (Scientific-Technical Project of the Deep-underwater Cubic-kilometer Scale Neutrino Telescope at Lake Baikal) (Moscow: INR RAS, 2010); http://baikalweb.jinr.ru/
16. Bagley P et al. (KM3NeT Collab.), KM3NeT Technical Design Report for a Deep-Sea Research Infrastructure in the Mediterranean Sea Incorporating a Very Large Volume Neutrino Telescope (2010); http://www.km3net.org/KM3NeT-TDR
17. IceCube South Pole Neutrino Observatory, http://www.icecube.wisc.edu
18. Aartsen M G et al. (IceCube Collab.) *Phys. Rev. Lett.* **113** 101101 (2014)